Battery Cell Temperature Sensing Towards Smart Sodium-Ion Cells for Energy Storage Applications

Timothy A. Vincent
Cell Instrumenation Team, WMG
University of Warwick
Coventry, CV4 7AL, UK.
T.A.Vincent@warwick.ac.uk

Ivana Hasa
Electrochemical Materials Team
WMG, University of Warwick
Coventry, CV4 7AL, UK.
Ivana.Hasa@warwick.ac.uk

Begum Gulsoy
Cell Instrumenation Team, WMG
University of Warwick
Coventry, CV4 7AL, UK.
Begum.Gulsoy.1@warwick.ac.uk

Jonathan E.H. Sansom
Cell Instrumenation Team, WMG
University of Warwick
Coventry, CV4 7AL, UK.
J.Sansom@warwick.ac.uk

James Marco
Cell Instrumenation Team, WMG
University of Warwick
Coventry, CV4 7AL, UK.
James.Marco@warwick.ac.uk

Battery cell instrumentation (e.g., temperature, voltage and current sensing) is vital to understand performance and to develop/contrast different cell designs and chemistries. Sodium-ion batteries (NIBs) are emerging as an alternative solution to lithium-ion (LIB) technology, particularly in the field of grid energy storage. The relative abundancy of sodium (Na) and superior charge/discharge capability, fuel the development effort to match the desirable energy density properties of LIBs. Internal temperature sensing is of particular value during cell development, offering insights into hot spots and manufacturing defects, in-advance of detection via voltage or surface temperature measurement. We developed novel thermistor arrays (7x miniature sensors) inserted into the core of a 21700 format LIB via flexible PCBs. These arrays were protected using a covering tube, and successfully provided temperature measurements throughout an ageing experiment consisting of 100 cycles (1C charge, 0.3C discharge). For the first time, we report on our performance tests prior to this ageing study (capacity, internal resistance) to highlight the instrumented cells show comparable degradation (~5 %) to an unmodified cell. We extend this study by verifying that our scalable low-cost solution to sensor protection can be migrated to NIBs. The resilience of the protected PCBs to electrolyte was tested via a longer-term test (preliminary results from a 90-day study are reported here) submerged within the solution. The findings offer a promising outlook to lower-cost cell instrumentation and will provide a tool to optimize these novel cell chemistries.

Keywords—Thermistor instrumentation, ageing, Na-ion batteries

I. INTRODUCTION

In the energy storage field, batteries are key to the deployment of electric vehicles (EVs). With the shift to renewable energy sources (e.g. solar, wind), there is increasing demand for storage systems to enable output to energy grids to be maintained, regardless of the variability of the output from the energy source [1]. Batteries offer a flexible and efficient solution to this energy storage problem, replacing traditional techniques (such as pumped hydroelectric, phase change or compressed air energy storage) [2].

It is recognised the use of rare-earth elements as part of the construction of lithium-ion batteries (LIBs), for example Lithium and Cobalt, limits production volume [3, 4]. These expensive elements will also prohibit the cost per kWh from reducing to levels desired for large-scale energy grid storage [5]. Sodium-ion batteries (NIBs), constructed of abundant elements, offer a pathway to reduced cost batteries [5, 6]. NIBs are particularly suited to stationary energy storage needs, where quick response times (i.e. fast discharge rates), resilience to ambient temperature shifts and reduced lifetime cost are desired [7]. Projected increases in energy density could also see NIBs introduced in the EV market, where their growing demand is putting pressure on LIB supply [5].

Battery packs rarely contain sufficient temperature sensors to monitor the condition of an individual cell (in the automotive industry, typically a pack with hundreds of cells may contain fewer than 20 sensors [8]). Traditional sensing methods involve complex wiring and are challenging to integrate into the pack, eventually leading to a trade-off between instrumentation density, monitoring ability and cost [9]. The battery management system (BMS) must therefore control the pack with limited data, relying on models to predict pack performance (e.g. state of charge, SoC) [10]. This is relatively well understood when the pack is at the start of its life, but ability to model cell parameters (capacity, voltage, etc.) degrades as the cells age; properties of an individual cell do not always scale when inserted at a system level [11].

To understand the performance of a battery cell, regardless of chemistry type, internal temperature sensors offer a valuable insight [12]. Internal temperature measurements decouple the effect of ambient conditions, where the cell skin is the thermodynamic boundary between the cell and its environment. This allows the effect of the ambient conditions on the core of the cell (i.e. the cooling/heating system) to be quantified. Internal measurements can also provide a unique view of the health of the cell, where fluctuations or hot spots in the cells can provide early indicators of cell failure [9, 13].

Promoting NIBs to the popularity of LIBs will come from integrating existing process and techniques, developed for the counterpart technology, with the upcoming chemistries. In this work we demonstrate our thermistor sensors, developed for 21700 format cylindrical LIBs, offer excellent sensing performance, and minimal impact on cell functionality, with results reported from a preliminary 100 cycle ageing profile. This expands on our previous works, detailing the instrumentation process [14]. This study is divided into two parts, firstly demonstrating the functionality of our sensors in commercial LIBs over a longer-term study; secondly, we complete the initial steps to prove this technology and processes can be transferred over to NIBs.

For the first time, we report on our study ageing LIBs instrumented with thermistor sensors (presented as a comparison with unmodified cells). We then complete a

Funding was received from the European Union's Horizon 2020 research and innovation program under Grant no. 883753 (SIMBA project). Funding was also received from the High Value Manufacturing Catapult, grant reference 160080 CORE, titled 'Smart Sensing for Future Batteries'.

preliminary assessment, by verifying reliable operation over a preliminary 90 day trial, to test if our unique sensors can be migrated over to NIB technology. Our initial experimentation reported here, investigates the low-cost protective coverings needed to protect the sensors, when submerged in sodium-ion electrolyte filled vials. This electrolyte is composed of a $NaPF_6$ (sodium hexafluorophosphate) salt dissolved in a mixture of solvents including ethylene carbonate (EC) and diethylene carbonate (DEC), similar in nature to standard electrolytes employed in LIBs. To the authors' knowledge, this novel research promotes opportunities to produce sensors capable of viable scalable production which has not been published previously. Current state-of-the-art literature details sensors protected with small-scale methodology (higher cost and relatively specialist), suitable only for laboratory trials [15]. Such sensors are designed for single-use, low-volume (a handful of cells). Here, we demonstrate our unique sensor arrays, designed with the aim to reproducibly instrument cells in small production runs. These batches of cells can be used to aid cell chemistry and cooling system development.

This paper is structured as follows: the background material introduces our literature findings and prior research leading to our decisions relating to cell instrumentation; our methodology details the process and techniques used in our cell instrumentation and testing procedures; we then present our results and discuss our findings. We then conclude our work and highlight the next key steps in our research.

II. Background

Currently NIBs lag behind LIBs in terms of energy density (at best, perhaps 150 Wh/kg versus 200 Wh/kg) [16]), thus current state-of-the-art NIBs match only lower range LIBs. Therefore at this stage, LIBs are preferred for applications requiring lighter weight, higher energy density batteries (i.e. transportation applications) [17]. NIBs have the potential to match the energy density of LIBs; critically for energy grid applications, they already offer excellent discharge properties (10 C rate typical, with up to 500 C tested) [7, 16, 17].

Furthermore, the environmental impact of cells after their first life must be considered; NIBs offer superior recycling capability, for example aluminium (Al) foils can be used for the current collectors (replacement for copper, Na does not alloy with Al [18]) for both the cathode and anode. This simplifies the recycling process, as Al foils are simpler to separate than copper [7]. Safer transportation is also possible (transport without damage possible at 0 V). NIB recycling is currently only studied at the laboratory scale, as their low production volumes neglect the need for volume recycling plants [7]. The current outlook offers promising opportunities to recycle NIBs [19], where knowledge and processes are set to be easily transferred from the more-mature LIB market.

Cylindrical cells - where the anode, separator and cathode are wrapped around (forming the 'jellyroll') which is then enclosed within an Al can - have a complex thermal structure, in-part due to their construction, involving materials of varying thermal conductivities. In the x-plane (radial) direction it is estimated this conductivity is around 1 W/m/K [15], although of course this is strictly dependent on the construction of the cell and materials [20], thus care must be taken when relying on surface temperature measurements. In pouch cells, thermal conductivity measurements demonstrate variability between manufacturers (e.g. 1.2 to 1.6 W/m/K cross-plane [21]); it has been shown these values decrease during cell cycling [21]. This uncertainty propagates to the BMS and thermal management system, where models used to predict state-of-charge cannot function optimally without reliable and well-understood sensor data.

Internal cell instrumentation offers a direct means of acquiring data to support pack development activities. Measurements of cell impedance (i.e., Electrochemical Impedance Spectroscopy, EIS) are a non-direct, non-invasive method of understanding cell condition [13]. Although EIS avoids damage or modification to cells, it is chemistry and design sensitive (thus a model must be developed for each cell type – a time consuming process, which should include cell ageing). Our research can encompass both prototyping work as well as supporting end applications (when monitoring is vital, in less cost-sensitive industries, e.g. aerospace). In terms of temperature sensing, previous works have demonstrated thermocouple [22], fibre optic [12, 23, 24] and thermistor [25] based systems. These are typically tested with LIBs, inside either cylindrical or pouch format cells. Thermocouple sensors are traditionally favoured, for easy integration with existing data acquisition equipment. However, these sensors provide only point measurements, and cannot be connected in series (each needs a reference cold junction).

Fibre optics offer distributed sensing (e.g. 2.6 mm spatial resolution [26]), thus can provide a detailed temperature map. Their fragility and relatively high cost currently restrict their use to laboratory experimentation; although their long sensing length (e.g. 5 m) allows multiple cells to be measured with a single fibre. To provide distributed measurements, costly equipment is needed to precisely perform measurements at high resolution and sample rate. Previous works in the field have instrumented cells in laboratory trials, involving manual processing and non-repeatable steps (such as hand machining and gluing) [24, 27], which limits the process scalability.

Thermistor based sensing offers a low-cost alternative (sensors available from $0.10), while permitting parallel connection of sensors, thus distributed sensing is possible; albeit 10 mm resolution reported in our previous work [14]. Our method of cell instrumentation has previously been detailed [14], thus will only briefly be introduced here. This method overcomes imprecise sensor locations (e.g., in the designs reported previously [25]) and leads the way towards automating instrumentation for fabricating larger volumes.

Electrolyte has previously been acknowledged as presenting a harsh (corrosive) chemical environment [28]. Complex and expensive conformal coating methods are usually employed for lower volume production, such as Parylene coating [15]. This coating is non-standard for PCB fabrication and would be difficult to scale to underpin volume manufacturing. To the authors' knowledge, although the sensor designs discussed have been tested in LIBs, there is no evidence of examining sensor performance during complete electrolyte submersion. Completely submerging the sensors presents the worst-case scenario; at low SOCs in preliminary instrumentation work, no liquid electrolyte was observed in 21700 format LIBs during disassembly.

Protecting the sensors with a heat-shrinkable plastic tube was preferred in our previous work, testing with 21700 format LIBs [14]; the resulting thermistor array is shown in Fig. 1. This method provides both a chemical resistive barrier, and a physical barrier, preventing damage from friction when the sensors are inserted into the cell.

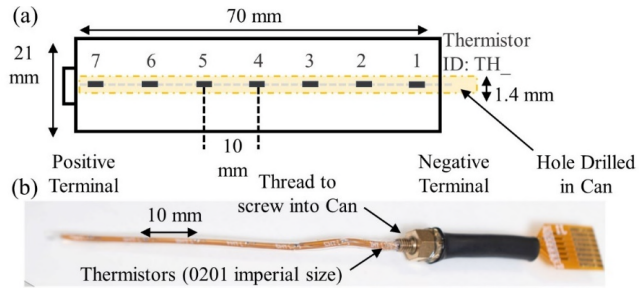

Fig. 1. Thermistor array designed for 21700 format cylindrical cell, (a) schematic layout for thermistors, (b) photograph showing completed flexible PCB with fitting to install into cell.

This method could be scaled up (for example rolling adhesive protective sheets on top of the sensor array); the plastic layer also provides good conformability around the rectangular edges of the thermistor sensors. Thus, if sensors were placed internally within a pouch cell, the covering will reduce the chance of sensors near the surface of the cell from piercing the foil bag or any sensors causing a short circuit (i.e. damaging the separator). However, the tubing does increase the bulk of the sensor arrays (wall thickness ~0.2 mm), consuming additional volume. Off-the-shelf liquid based conformal coatings may provide good protection against electrolyte; these options will be investigated in further work.

III. Methodology

Instrumented 21700 LIBs have been detailed in our previous work [14]. Briefly, the LIBs used in this work have a vacant volume in the core, remaining from the manufacturing process. To insert sensors into this core, the negative terminal of the cell was drilled and tapped via a flow drilling and flow tapping, respectively. These processes for a M2.5 thread in the AI can, with minimal damage to the cell (forming the hole and thread, not cutting) and without introducing metallic swarf/debris into the jelly-roll. A reference performance test (RPT), detailed previously, measures the capacitance and DC resistance of the cell; these values are compared at various stages (see Results section) from pre-instrumentation to after an ageing cycle of 100 cycles. Three cells fitted with thermistor sensors were fabricated, along with three unmodified reference cells.

Sensors for instrumentation and the fittings were prepared and constructed entirely prior to installation in the cell. The drilling process and sensor insertion was performed in an argon environment glovebox, <10 ppm moisture. The flexible PCBs were populated (0201 imperial sized thermistors), and then covered with the transparent protective heat-shrinkable tubing. A brass fitting (M2.5 thread with hex shape for tightening) is installed 70 mm away from the end of the array, and secured via a second heat shrinkable tube (black tubing, Fig. 1) – this ensures the sensors were placed precisely and reproducibly, without needing to perform measurements when wearing cumbersome gloves in a glovebox. Tabbed cells are used in this work, where typical cell holders (e.g. with spring loaded pins) cannot accept cells with sensors inserted. Tabbing cells is often preferred, to obtain the lowest possible contact resistance and tighter tolerances. In future work we aim to design an improved cell end-cap, to allow a flush finish to the cell. We propose instrumented cells can be integrated within a module design, thus the cells may not be tabbed during the instrumentation. In this way, our finalised process must be agnostic; either stand-alone with tabs (for individual cell testing) or if tabs are to be welded post-instrumentation.

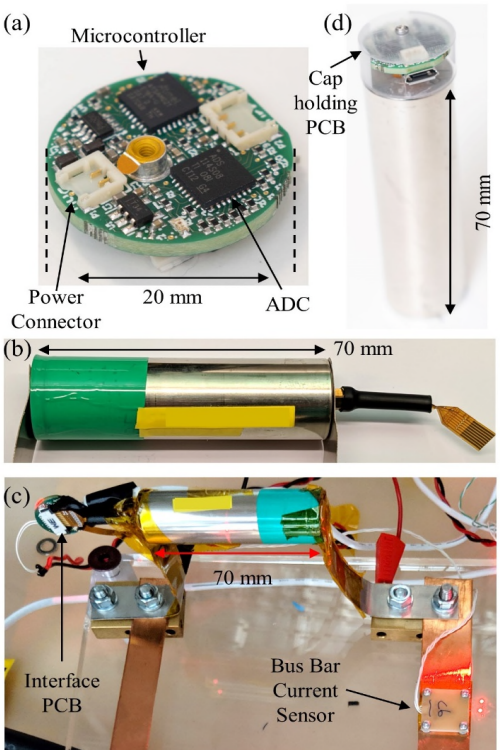

Fig. 2. Photographs of assembled instrumented cell, (a) populated interface PCB, (b) completed instrumented cell with thermistor array, (c) instrumented cell with interface circuitry installed in ageing test rig, (d) concept smart cell cap, containing interface PCB.

The cells were subjected to an ageing profile (0.3C discharge, 1C charge) for 100 cycles, performed using a Digatron MCT 20-6-6/20-18-4 cycler. The ageing profile charged the cells to full capacity (4.2 V) and discharged the cells to 0 % SoC (2.5 V), with both discharge/charge stages operating constant current – constant voltage. Minimal rest period (1 min) was allowed between each discharge/charge step and each cycle. Capacity measurements were taken by performing the RPT every 20 cycles, with all experiments performed within a climatic chamber (25 °C constant). This extends our previous studies [14, 29], where the cells were tested for periods of <50 cycles, without capacity measurement. The sensor reliability and possible impact on the cell performance were not comprehensively assessed.

Data from the thermistors were recorded using a custom miniature PCB, Figure 2 (a). The assembled instrumented cell is shown in Fig. 2 (b); the cell is installed in a test rig (c), which is allows battery cycler channel cables to be connected for the ageing cycling experiments. In addition to the internal thermistor sensing, a prototype bus-bar current sensor is installed for each cell (detailed in previous works [14, 29]). A concept smart cell (an intermediary design, incorporating the flexible PCB and interface PCB secured in a cap) is shown in Fig. 2 (d). The interface PCB, detailed previously [14, 29], incorporates a 16-bit ADC (TI ADS114s08), and a microcontroller (SAMD21E) to allow data logging via a USB connection, without requiring additional apparatus. The PCB also incorporates a powerline communication (PLC) modem to allow data to be transferred at high frequency along the cell bus-bars; this feature is not tested here. A detailed description of its design and verification can be found in our previous work [29]. Each cell is connected singly to a cycler channel, thereby PLC data would need to be extracted from each pair of bus-bars individually, involving greater complexity of

cabling compared to using a traditional wired cable. PLC is preferred for module testing, where data from a range of cells can be accessed over a single bus bar.

The LIB ageing study will form the basis to produce cell sensors agnostic to chemistry type, suitable for benchmarking cell designs. In this part of the study, sensor arrays were submerged in vials of the $NaPF_6$ electrolyte. This enabled the resilience of the tubing to be assessed, while also decoupling any reaction between the sensor material and cell performance. I.e., it is important also to verify there is no effect on the chemical solution, such as debris being deposited as a result of the selected covering method.

In preliminary work, failing thermistor arrays were noted to produce spurious results, with erroneous peaks. To eliminate environmental temperature effects, the vials were placed in a block heater (Techne DB100/2TC), maintained at a constant temperature of 25 °C. Sensors TH6 and TH7 (schematic Fig. 1) only were populated on each PCB, providing 2 data points per array, as shown in Fig. 3 (a). Two arrays (each in a separate vial) were tested for each of the following scenarios: (i) uncoated PCB, (ii) Tube covered PCB, (iii) Parylene coated PCB. 10 kΩ nominal (25 °C) thermistors were used for arrays (i) and (ii), whereas 100 kΩ thermistors were used for design (iii). Due to the long-lead times and cost associated with design (iii), a replacement design with identical thermistors to the other designs could not be fabricated. Higher resistance thermistors were previously selected for cell instrumentation to ensure the lowest possible current requirement, while also presenting a larger change in resistance to a given temperature change. A larger magnitude response allows lower-cost components (i.e. ADC and associated passive components) to be substituted in future revisions. In these studies, precision and accuracy of response is preferred, governing the choice of a high-resolution ADC, with buffered inputs. Two reference thermocouples were placed in separate vials in the block, shown in Fig. 3 (b).

Fig. 3. Sensors in vials prepared for electrolyte submersion, (a) two thermistors populated per PCB, (b) vials placed in block (constant 25 °C).

IV. Results & Discussion

A. LIB Cell Instrumentation and Ageing

Principally in this study, we consider the cell capacity measurement (coulomb counting via the cycler) as a measure of cell degradation. To ensure there is minimal damage to the internal current collector when the M2.5 thread is formed, the direct current internal resistance (DCIR) of the cell is also measured. Table 1 summarises the capacity lost for each cell between pristine condition (first RPT), post-modification (sensor inserted where applicable) and then after 100 ageing cycles. Fig. 4 shows the capacity loss following each 20 ageing cycles. Table 2 presents the corresponding DCIR data.

TABLE I. Capacity measured for cells, pre- and post-instrumentation and following ageing profile of 100 cycles. TH- Thermistor instrumented cell; UN- unmodified cell.

Cell Type	*Capacity [Ah] (RPT 1)*	*Capacity post-instr [Ah]*	*Capacity after 100 cycles [Ah]*	*Capacity loss (100 cycles) [%]*
TH (1)	4.84	4.80	4.55	5.49
TH (2)	4.85	4.81	4.56	5.48
TH (3)	4.86	4.83	4.57	5.69
UN (1)	4.83	-	4.57	5.69
UN (2)	4.83	-	4.57	5.69
UN (3)	4.80	-	4.56	5.26

TABLE II. DCIR of cells measured, pre- and post-ageing study (measurements taken at 100 % SoC).

Cell Type	*DCIR (pre-ageing) [mΩ]*	*DCIR (post-ageing) [mΩ]*	*DCIR Increase [mΩ] (%)*	*DCIR Overall Std. Dev. [mΩ]*
TH (1)	30.05	32.80	2.75 (9.1 %)	0.85
TH (2)	29.03	32.00	2.97 (10.2 %)	0.96
TH (3)	29.27	31.91	2.64 (9.0 %)	1.15
UN (1)	27.90	31.30	3.40 (12.2 %)	1.28
UN (2)	28.40	31.50	3.10 (10.9 %)	1.08
UN (3)	28.90	31.80	2.90 (10.0 %)	1.05

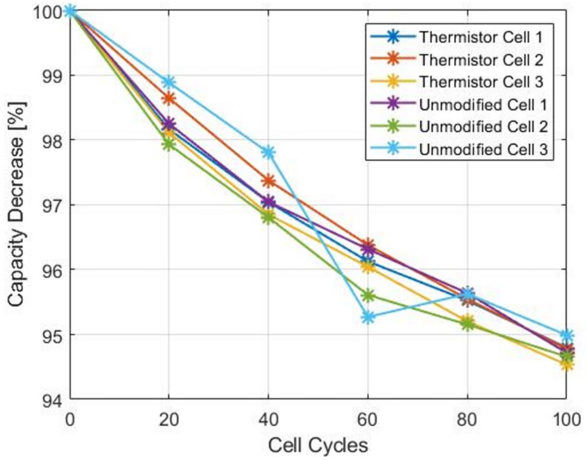

Fig. 4. Sensors Capacity loss (percentage from start of ageing profile) for 3x thermistor instrumented cells and 3x unmodified cells.

The thermistor instrumented cells demonstrate comparable performance to the unmodified cells, where average capacity loss during the 100 cycles was 5.55 % - the pristine cells lost 5.54 %. This is supported by previous data in the literature for LIBs, where typically between 5 to 6 % capacity loss was reported by Atalay et al., cycling 0.33 C charge and 1 C discharge [30]. The average DCIR increase during the 100 cycles was 2.79 mΩ (9.4 %) for the instrumented cells, compared to 3.13 mΩ (11.0 %) for the unmodified cells. The standard deviation data demonstrates the unreliable nature of measurement technique, where an error of around 1 mΩ is found regardless of cell type. This error is likely introduced by a number of factors, for example, the physical connections to the cycler (brass blocks and tabs used) or the voltage acquisition accuracy of the equipment (to record the profile following the pulse discharge used for DCIR measurement). The data is sufficient however to conclude there is no significant difference in performance compared to the unmodified cells. To verify the sensors remain operational throughout the ageing cycling profile, data were logged from the thermistor sensors continuously at a measurement rate of 1 Hz. An 800 min section of the data extracted from the first (a) and final (b) 20 cycle profiles are presented in Fig. 5.

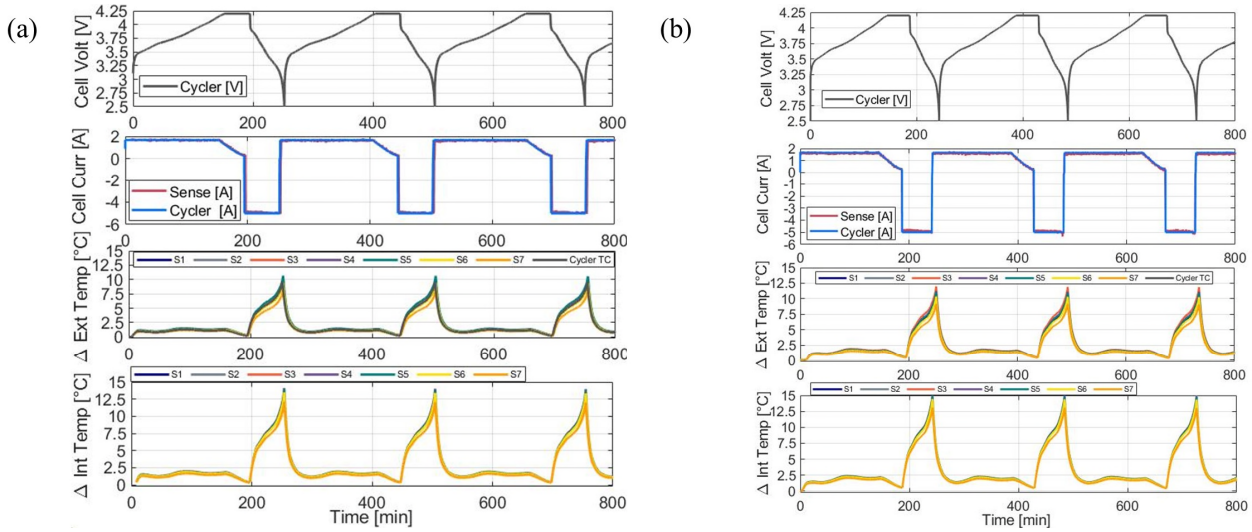

Fig. 5. Sensor data logged during the ageing study, consisting of current, internal temperature and surface temperature, with (a) data acquired during cycles 1 to 3, and (b) data acquired during the cycles 81 to 83. S1 to S7 refer to thermistors TH1 to TH7, arranged along the surface and internally inside the cell.

The peak temperatures occur following the 1C discharge phase for each cycle. During the stages of cycles 0 to 20 and 80 to 100, internal sensors TH3 and TH4 exhibit the highest temperature readings (14.0 and 15.1 °C increases above ambient 25 °C, respectively). Similarly, the RPT (measurement of capacity/DCIR) post-ageing demonstrated a higher increase in temperature compared to the first RPT performed pre-ageing (data not shown here). These peak temperatures occur after a similar 1C discharge; values of approx. 10 °C increase above ambient are expected (reported in our previous work [14]). In this scenario, an elevated peak temperature was noted (TH7 ~ 13.8 °C) again indicating the ageing cell produces greater heat during discharge, potentially caused by an increased internal resistance.

B. Na Electrolye Experimentation

The coated sensor array configurations (i) to (iii) were submerged in electrolyte filled vials for a period of 90 days. Data were recorded in the heater block, (constant 25 °C). Raw resistance data are shown in Table 3; following the 90 day period the thermistor arrays were removed from the heater block prior to the resistance values being recorded.

TABLE III. SENSOR DATA SUBMERGED IN ELECTROLYTE. NC – NONCOATED, TB- TUBE COVERED, PL -PARYLENE COATED, TC – THERMOCOUPLE, NORD- NO READING POSSIBLE.

Design	*Initial TH6/TH7 [kΩ]*	*Day 5 TH6/TH7 [kΩ]*	*Day 90 TH6/TH7 [kΩ]*
(i) NC 1	10.42/10.41	8.86/8.04	NoRd/NoRd
(i) NC 2	10.51/10.49	9.28/9.67	NoRd/NoRd
(ii) TB 1	10.49/10.53	10.39/10.41	NoRd/10.92
(ii) TB 2	10.61/10.49	10.62/10.53	11.06/11.16
(iii) PL 1	107.72/105.89	107.32/103.55	109.96/102.12
(iii) PL 2	105.41/105.48	105.87/105.23	112.16/111.88
TC1/2	~25 °C	~25 °C	~25 °C

The non-protected PCBs fail within the 5 day period, with resistances dropping below 9 kΩ (theoretically indicating a temperature > 30 °C). The reaction must be verified further, where an increase in resistance would typically indicate damage to the PCB conductive tracks, opposed to the decrease observed. Following the 90 day period, the resistance could not be measured (i.e. open circuit). TH6 on the TB 1 PCB notably also failed to produce a reading after the 90 day duration (open circuit also measured for this thermistor). The cause of failure could not be identified through visual inspection. This indicates the need for detailed inspection of solder joint quality during component population. TB1 and TB2 produced no visible effect on the electrolyte solution, potentially indicating no reaction with the chemicals. The vial in which PL2 was submerged was noted to contain debris at the end of the experiment. This data strengthens our aim to find a thin conformal coating, that provides chemical resilience with no detrimental effect on cell operation.

V. CONCLUSIONS AND FURTHER WORK

Emerging battery chemistries, such as Na-ion, are set to build upon the rapid advances in LIBs, while overcoming the shortage of raw materials that will halt the desired downward trend in cost per kWh. NIBs are of particular interest in grid energy storage, where renewable energies (solar, wind, etc.) often provide inconsistent production, thereby requiring a ready store of energy for immediate deployment to the grid when demand dictates. Extreme discharge rates, perhaps order of magnitude greater than with LIB, are realistic with NIBs.

Instrumenting cells, e.g. core thermistor temperature sensors, offers unique insights. It is proposed earlier warning of cell failure and improved understanding of cooling system design can be gained. In this work we further our previous studies with short term cycling, and report upon an ageing profile of 100 cycles (0.3 C charge, 1 C discharge). The cylindrical cells were instrumented using our unique drilling process, minimising damage to the cell, while providing a repeatable and robust means to install sensors (low volumes of cells). The operation of the cell was assessed in terms of capacity fade and DC resistance, then compared to unmodified cells. The instrumentation had negligible effect on cell performance (capacity fade ~5.5 %, identical to the reference cells), and a DCIR increase of < 10 % after ageing was less than that for the unmodified cells (11 %).

To ensure our sensor systems and processes are chemistry agnostic, and suitable for future NIB cells, the sensor coverings were tested for resilience against a $NAPF_6$ based electrolyte. To examine both the coverings resilience to the

solution, as well as verifying the mixture was not contaminated by the sensors, the PCB thermistor arrays were submerged in vials of the electrolyte. These vials were kept at constant temperature in a block heater (25 °C). The tube covered design, verified with LIBs, was tested with a reference Parylene coated PCB and an uncoated PCB. The boards were left submerged for a period of 90 days, with measurements taken at 0, 5 and 90 day points. The uncoated PCBs failed within the first 5 days, exhibiting theoretical temperature readings above 30 °C (a drop in ~ 1 kΩ/10% resistance), which was not observed with the Parylene reference thermistors nor thermocouple sensors. After the 90 day period, the Parylene coated devices functionality was verified, correctly reading temperature at 25 °C, however one PCB was noted to leave debris in the vial. The tube coated PCBs did not contaminate the solution, but one sensor failed during the experiment. We conclude the tube covering offers a proven method for instrumenting cylindrical cells, although less bulky coverings are desired to reduce the volume consumed inside the cell.

Further work involves a complex test matrix of $NaPF_6$ conformal coating experimentation. This proof-of-concept data has demonstrated a conformal coating is needed, and an unprotected PCB will fail quickly. A revised setup will include logging at regular intervals (i.e. 1 min) over a period of weeks. Thinner (and scalable to production) conformal coatings will be tested, with both the operation of the PCB and purity of the electrolyte monitored. The LIB ageing work will continue, with the cells cycled for 100 additional cycles.

REFERENCES

[1] F. Díaz-González et al., "A hybrid energy storage solution based on supercapacitors and batteries for the grid integration of utility scale photovoltaic plants," J. Energy Storage, vol. 51, p. 104446, Jul. 2022, doi: 10.1016/J.EST.2022.104446.

[2] W. Yu, Y. Liu, L. Liu, X. Yang, Y. Han, and P. Tan, "Rechargeable aqueous Zn-LiMn2O4 hybrid batteries with high performance and safety for energy storage," J. Energy Storage, vol. 45, p. 103744, Jan. 2022, doi: 10.1016/J.EST.2021.103744.

[3] L. S. Martins, L. F. Guimarães, A. B. Botelho Junior, J. A. S. Tenório, and D. C. R. Espinosa, "Electric car battery: An overview on global demand, recycling and future approaches towards sustainability," J. Environ. Manage., vol. 295, p. 113091, Oct. 2021, doi: 10.1016/J.JENVMAN.2021.113091.

[4] M. Mohr, J. F. Peters, M. Baumann, and M. Weil, "Toward a cell-chemistry specific life cycle assessment of lithium-ion battery recycling," J. Ind. Ecol., vol. 24, 2020, doi: 10.1111/JIEC.13021.

[5] P. K. Nayak, et al., "From Lithium-Ion to Sodium-Ion Batteries: Advantages, Challenges, and Surprises," Angew. Chemie - Int. Ed., vol. 57, no. 1, pp. 102–120, Jan. 2018, doi: 10.1002/ANIE.201703772.

[6] H. S. Hirsh, Y. Li, D. H. S. Tan, M. Zhang, E. Zhao, and Y. S. Meng, "Sodium-Ion Batteries Paving the Way for Grid Energy Storage," Adv. Energy Mater., vol. 10, Aug. 2020, doi: 10.1002/AENM.202001274.

[7] T. Liu et al., "Exploring competitive features of stationary sodium ion batteries for electrochemical energy storage," Energy Environ. Sci., vol. 12, no. 5, pp. 1512–1533, May 2019, doi: 10.1039/C8EE03727B.

[8] T. Grandjean, A. Barai, E. Hosseinzadeh, Y. Guo, A. McGordon, and J. Marco, "Large format lithium ion pouch cell full thermal characterisation for improved electric vehicle thermal management," J. Power Sources, vol. 359, 2017, doi: 10.1016/j.jpowsour.2017.05.016.

[9] R. R. Richardson, S. Zhao, and D. A. Howey, "On-board monitoring of 2-D spatially-resolved temperatures in cylindrical lithium-ion batteries, vol. 327, 2016, doi: 10.1016/j.jpowsour.2016.06.104.

[10] M. F. Niri, T. M. N. Bui, T. Q. Dinh, E. Hosseinzadeh, T. F. Yu, and J. Marco, "Remaining energy estimation for lithium-ion batteries via Gaussian mixture and Markov models for future load prediction," J. Energy Storage, vol. 28, Apr. 2020, doi: 10.1016/j.est.2020.101271.

[11] T. Bruen and J. Marco, "Modelling and experimental evaluation of parallel connected li-ion cells for an electric vehicle battery system," J. Power Sources, vol. 310, 2016, doi: 10.1016/j.jpowsour.2016.01.001.

[12] A. Fortier, M. Tsao, N. D. Williard, Y. Xing, and M. G. Pecht, "Preliminary study on integration of fiber optic bragg grating sensors in li-ion batteries and in situ strain and temperature monitoring of battery cells," Energies, vol. 10, no. 7, 2017, doi: 10.3390/en10070838.

[13] M. Ströbel, J. Pross-Brakhage, M. Kopp, and K. P. Birke, "Impedance Based Temperature Estimation of Lithium Ion Cells Using Artificial Neural Networks," Batter. 2021, Vol. 7, Page 85, vol. 7, no. 4, p. 85, Dec. 2021, doi: 10.3390/BATTERIES7040085

[14] T. A. Vincent, B. Gulsoy, J. E. H. Sansom, and J. Marco, "In-situ instrumentation of cells and power line communication data acquisition towards smart cell development," J. Energy Storage, vol. 50, p. 104218, Jun. 2022, doi: 10.1016/J.EST.2022.104218.

[15] G. Zhang, et al., "In Situ Measurement of Radial Temperature Distributions in Cylindrical Li-Ion Cells," J. Electrochem. Soc., vol. 161, no. 10, pp. A1499–A1507, Jul. 2014, doi: 10.1149/2.0051410.

[16] K. Chayambuka, G. Mulder, D. L. Danilov, and P. H. L. Notten, "From Li-Ion Batteries toward Na-Ion Chemistries: Challenges and Opportunities," Adv. Energy Mater., vol. 10, no. 38, Oct. 2020, doi: 10.1002/AENM.202001310.

[17] C. Y. Yu et al., "NaCrO2 cathode for high-rate sodium-ion batteries," Energy Environ. Sci., vol. 8, no. 7, pp. 2019–2026, Jul. 2015, doi: 10.1039/C5EE00695C.

[18] I. Hasa et al., "Challenges of today for Na-based batteries of the future: From materials to cell metrics," J. Power Sources, vol. 482, p. 228872, Jan. 2021, doi: 10.1016/J.JPOWSOUR.2020.228872.

[19] D. Karabelli et al., "Sodium-Based Batteries: In Search of the Best Compromise Between Sustainability and Maximization of Electric Performance," Front. Energy Res., vol. 8, p. 349, Dec. 2020, doi: 10.3389/FENRG.2020.605129.

[20] K. J. Lee, K. Smith, A. Pesaran, and G. H. Kim, "Three dimensional thermal-, electrical-, and electrochemical-coupled model for cylindrical wound large format lithium-ion batteries," J. Power Sources, vol. 241,. 2013, doi: 10.1016/j.jpowsour.2013.03.007.

[21] H. Maleki, H. Wang, W. Porter, and J. Hallmark, "Li-Ion polymer cells thermal property changes as a function of cycle-life," J. Power Sources, vol. 263, 2014, doi: 10.1016/j.jpowsour.2014.04.033.

[22] C. Xu et al., "Internal temperature detection of thermal runaway in lithium-ion cells tested by extended-volume accelerating rate calorimetry," J. Energy Storage, vol. 31, p. 101670, Oct. 2020, doi: 10.1016/J.EST.2020.101670.

[23] E. Vergori and Y. Yu, "Monitoring of Li-ion cells with distributed fibre optic sensors," in Procedia Structural Integrity, 2019, vol. 24, pp. 233–239, doi: 10.1016/j.prostr.2020.02.020.

[24] Y. Yu, E. Vergori, F. Maddar, Y. Guo, D. Greenwood, and J. Marco, "Real-time monitoring of internal structural deformation and thermal events in lithium-ion cell via embedded distributed optical fibre," J. Power Sources, vol. 521, p. 230957, Feb. 2022, doi: 10.1016/J.JPOWSOUR.2021.230957.

[25] J. Fleming, T. Amietszajew, J. Charmet, A. J. Roberts, D. Greenwood, and R. Bhagat, "The design and impact of in-situ and operando thermal sensing for smart energy storage," J. Energy Storage, vol. 22, no. October 2018, pp. 36–43, 2019, doi: 10.1016/j.est.2019.01.026.

[26] Y. Yu, T. Vincent, J. Sansom, D. Greenwood, and J. Marco, "Distributed internal thermal monitoring of lithium ion batteries with fibre sensors," J. Energy Storage, vol. 50, p. 104291, Jun. 2022, doi: 10.1016/J.EST.2022.104291.

[27] S. Novais et al., "Internal and External Temperature Monitoring of a Li-Ion Battery with Fiber Bragg Grating Sensors," Sensors, vol. 16, no. 9, p. 1394, Aug. 2016, doi: 10.3390/s16091394.

[28] F. Saidani, et al., "A lithium-ion battery demonstrator for HEV applications featuring a smart system at cell level," in 2017 IEEE International Symposium on Systems Engineering, ISSE 2017 - Proceedings, 2017, doi: 10.1109/SysEng.2017.8088249.

[29] T. A. Vincent, B. Gulsoy, J. E. H. Sansom, and J. Marco, "A Smart Cell Monitoring System Based on Power Line Communication—Optimization of Instrumentation and Acquisition for Smart Battery Management," IEEE Access, vol. 9, pp. 161773–161793, Nov. 2021, doi: 10.1109/ACCESS.2021.3131382.

[30] . S. Atalay, et al., "Theory of battery ageing in a lithium-ion battery: Capacity fade, nonlinear ageing and lifetime prediction," J. Power Sources, vol. 478, 2020, doi: 10.1016/J.JPOWSOUR.2020.229026